Proceedings of Meetings on Acoustics

Volume 14, 2011 http://acousticalsociety.org/

162nd Meeting
Acoustical Society of America
San Diego, California
31 October - 4 November 2011

Session 4aNS: Noise

# 4aNS9. Low-frequency calibration of a multidimensional acoustic intensity probe for application to rocket noise

**Jarom H. Giraud*, Kent L. Gee, Scott D. Sommerfeldt, Troy Taylor and Jonathan D. Blotter**

***Corresponding author's address: Brigham Young University, Provo, Utah 84602, jaromgiraud@gmail.com**

Microphone arrays used to measure acoustic intensity and other energy quantities traditionally have low-frequency bandwidth limitations (e.g., below 100 Hz) thereby excluding the lowest, and in some cases, the most energetic frequencies generated by large rocket motors. At these low frequencies, the phase and magnitude mismatch between microphones becomes greater and the acoustic phase separation between any two microphones becomes smaller, resulting in more error in estimating the pressure gradients. To investigate the low-frequency response of an acoustic intensity probe, a turntable is used to rotate a four-microphone probe in a low-frequency noise field. An experimental assessment of the bandwidth is given for both magnitude and directional response down to approximately 40 Hz. The effectiveness of a microphone interchange calibration technique to remove amplitude and phase mismatch and increase the usable bandwidth of the probe is also discussed.

Published by the Acoustical Society of America through the American Institute of Physics

 [DOI: 10.1121/1.4817532]
Received 13 May 2013; published 22 Jul 2013
Proceedings of Meetings on Acoustics, Vol. 14, 040006 (2013)

## BACKGROUND

Large solid rocket motors, such as those used for sending equipment and personnel into space, generate intense acoustic levels during firing. For these larger motors (nozzle diameters ~1 to 3.5 m) low frequencies, on the order of tens of Hz, dominate the acoustic spectrum and peak pressures approach that of the atmosphere near the plume. These acoustic loads are capable of damaging near-by structures and are necessarily accounted for in the engineering of these launch vehicles and support structures. A typical spectral response near one of these motors is shown in Figure 1. Notice the amount of acoustic energy at frequencies as low as 10 Hz. This source spans the entire audible range at levels over 80 dB and has the most acoustic energy below 100 Hz, which is a difficult region to accurately measure acoustic intensity.

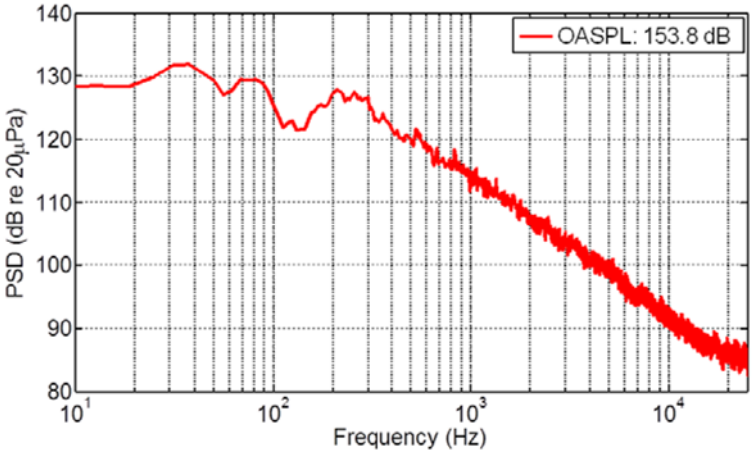


Figure 1.Typical spectra from a GEM-60 solid rocket motor (1.09 m nozzle diameter) at a location ~28 nozzle diameters downstream and ~18.5 nozzle diameters from the axis of firing.

The most common acoustic models for rocket noise prediction are the distributed source methods described in NASA report SP-8072[1]. These models attempt to predict rocket acoustics by modeling the exit plume as a series of discrete sources with an assigned amplitude and frequency content. The accuracy of this model is directly tied to the present day understanding of noise generation in a rocket plume. A goal of this research is to improve our accuracy of measuring acoustic intensity at both low and high frequencies to better understand and describe noise generation in the rocket plume and thereby improve these models.

The so-called "p-p" method for measuring acoustic intensity utilizes an approximation of the particle velocity from two pressure microphones and their average pressures to calculate acoustic intensity. This method relies on the accurate measurement of both magnitude and phase characteristics of an acoustic source.[2,3] While high-frequency intensity measurements are limited by scattering and increased errors in approximating collocated pressure and velocity, low-frequency measurements are limited by frequency response characteristics of the microphones used in the measurement. This paper describes the problem of inaccurate low-frequency microphone response, an approach for improving it and experimental verification of the method. Also included are suggestions for future research in this area.

Figure 2 shows a typical arrangement for performing the p-p method in one dimension. In this figure, two microphones separated by a distance, $\boldsymbol{d}$, measure acoustic intensity along a single dimension $\hat{\boldsymbol{x}}$ by approximation of the acoustic pressure and particle velocity at a point exactly

between the two sensors. As the spacing between sensors approaches a half wavelength, the approximation used to estimate the acoustic pressure at the geometric center of the array degrades. The closer two microphones are spaced, the higher in frequency the probe can measure accurately. However, as sensors are placed closer together, the low-frequency response becomes subject to phase mismatch between sensors as this mismatch becomes large relative to the acoustic phase separation of the sensors. Amplitude mismatch between sensors also becomes more influential as separation distance is decreased. To combat this and obtain a broadband measurement, multiple microphone spacings[4,5] are used during repeated measurements for repeatable measurements such as machine or room noise.

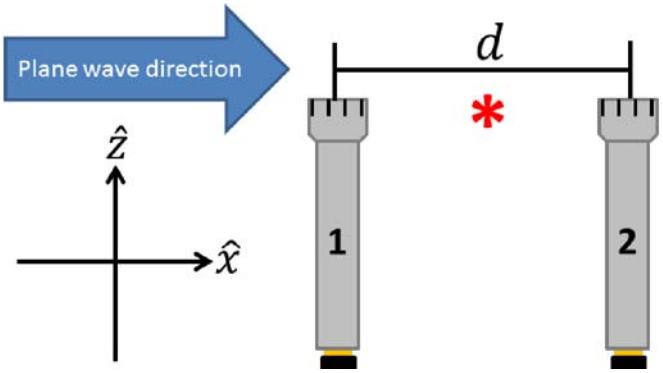


Figure 2. A typical setup for the p-p method.

When attempting to acquire broadband noise radiation data from a rocket motor, it is difficult (or impossible) to repeat the test after adjusting the spacing. As an alternative, an option is to place the sensors as close together as needed to obtain the high end of the desired bandwidth and try to minimize the low-frequency effects of phase and magnitude mismatch by means of a calibration. Maximizing bandwidth is a balance between microphone spacing, microphone frequency response, frequencies of interest, acceptable error and atmospheric considerations including sound speed and homogeneity of the field.

Microphones have mechanical, electrical and acoustical components that behave as inductive, capacitive or resistive elements. The combination of these components gives rise to high-pass filtering effects which causes roll-off in both magnitude and phase at low frequencies. Minor adjustments in venting, volume behind the microphone back plate, and other electronic, mechanical and acoustical discrepancies between sensors will alter this roll-off.[6] As a rule, no two manufactured microphones will have identical magnitude and phase response; this contributes to measurement uncertainty or error.

Consider two microphones used to perform the p-p intensity measurement with a separation distance of 2.54 cm. At 13.72 kHz and a sound speed of 343 m/s, the wavelength is 2.54 cm and the acoustic phase difference between the two microphones is 360°. As frequency decreases, this acoustic phase difference between microphones also decreases, as seen in Figure 3. For comparison, the phase error between two typical (un-matched) 6.35mm microphones is also included in this figure. In this two-microphone example, the microphones are aligned with preamps parallel to $\hat{z}$ and the separation is only along $\hat{x}$, as in Figure 2. The direction of plane wave propagation is also along the $\hat{x}$ direction.

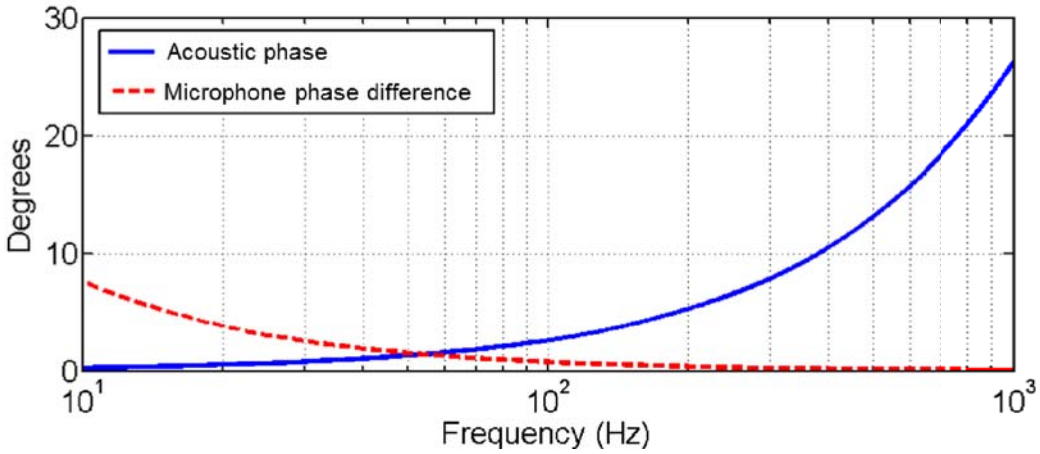


Figure 3. Representative trends of acoustic phase and the phase difference between two microphones separated by 2.54 cm. Acoustic phase difference between two microphones separated by some distance decreases proportional to frequency. The electro-mechanical phase difference between two similar microphones becomes large at low frequencies.

One may purchase manufactured "magnitude and phase matched" microphone pairs with variations in phase response measured as approximately < 0.2° for 20 Hz to 1 kHz and magnitude variations of < 0.2 dB for 20 Hz to 2 kHz[7]. For a two-microphone p-p probe it is the relative phase and magnitude error between sensors that determines the low-frequency end of the probe bandwidth. The effect of a constant phase error over frequency for a microphone spacing of 2.54 cm is seen in Figure 4.

Assuming two microphones are perfectly matched in magnitude response but have a phase difference of $\phi$, the intensity magnitude error as a function of frequency can be written[8] as

$$Error(Intensity) = 10\log_{10}\left[\frac{\sin(kd-\phi)}{kd}\right]. \quad (1)$$

This relationship is found by deriving acoustic intensity via the p-p method and modifying the phase of one sensor by $kd$, (wavenumber times microphone separation distance) the acoustic phase separation, and $\phi$, the assumed phase error between microphones. Figure 4 shows this relationship for the case of the one-dimensional plane wave as in Figure 2.

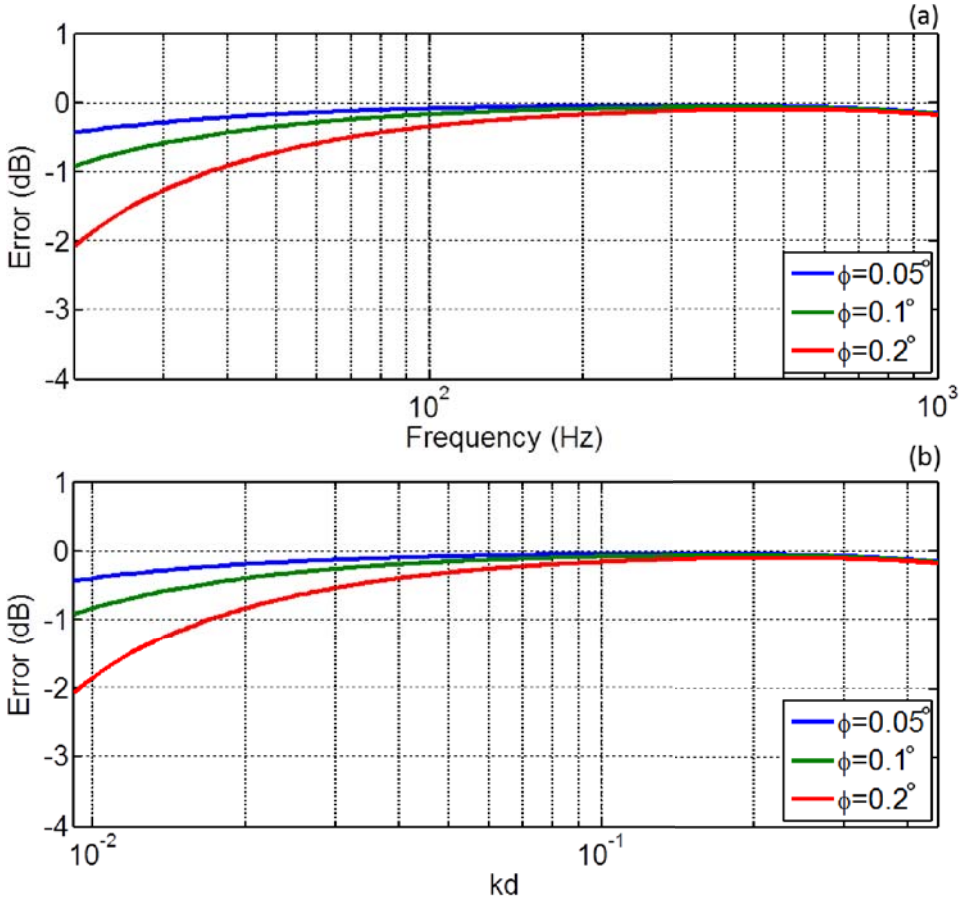


Figure 4. Error in measuring the intensity magnitude for various phase errors, $\phi$, between sensors (a) For two microphones separated by $d = 2.54$ cm. (b) For a dimensionless quantity $kd$, which relates frequency and separation distance (no longer fixed at 2.54 cm).

Although Figure 4 (a) is presented with frequency (in Hz) as the independent variable, this plot is easily transformed to the non-dimensionalized variable, *kd* (wavenumber times separation distance), as shown in Figure 4(b). A *kd* plot is useful because it allows one to determine a frequency limit for a given separation distance or determine a separation distance that allows for accurate measurement at a desired frequency.

## CALIBRATION

Any two microphones with a stable (however inaccurate) magnitude and phase response can be calibrated for use in a low-frequency intensity probe by using Chung and Blaser's switching technique.[9] This ability to calibrate (and re-calibrate) microphone sets is advantageous for use in measuring rocket noise because the response may be checked, after subjecting the sensors to the harsh environment created by a rocket, without sending the transducer back to the manufacturer. Also, the calibration can be performed before the test using a simple apparatus.

To remove the effects of magnitude and phase error between sensors, there are multiple calibration approaches using transfer functions.[10-13] The method employed in this thesis is the switching technique calibration by Chung and Blaser.[9] However, this calibration is obtained in the lab and not in-situ, such as demonstrated by Chung in other work.[11] Being able to calibrate

prior to the actual measurement is essential in making rocket noise measurements due to the inability of calibrating *in situ* with the source (rocket motor) to be tested.

The switching technique utilizes the geometric mean of two transfer functions to remove the effect of the field on the calibration. Consider two similarly shaped microphones in a sound field. Each microphone has a separate output, $\hat{e}_{I,1}$ and $\hat{e}_{I,2}$, (see Figure 5 for definitions) related to the acoustic pressure, microphone response, and electronic response. The ratio of the outputs is a transfer function, $H$, between microphones. This relationship may be processed in the frequency domain as a ratio of cross-spectra, $G$,

$$H_{I,12} = \frac{\hat{e}_{I,2}}{\hat{e}_{I,1}} = \frac{G_{I,12}}{G_{I,11}}. \quad (2)$$

If the locations of these sensors are exactly reversed, as in Figure 5, and the remainder of the measurement field remains unchanged, a second measurement and resulting transfer function may be obtained as

$$H_{II,12} = \frac{\hat{e}_{II,2}}{\hat{e}_{II,1}} = \frac{G_{II,12}}{G_{II,11}}. \quad (3)$$

Then, by taking the geometric mean of the two transfer functions obtained, a new transfer function is obtained that relates the two microphone responses by

$$H_{cal,12} = \sqrt{H_{II,12}H_{I,12}}. \quad (4)$$

To apply the calibration, one then multiplies $H_{cal,12}$ by $\hat{e}_{I,2}$ and the p-p intensity method may be performed in the usual fashion. This method modifies the response of the second microphone to match what the first microphone would have measured in the same location with the same stimulus. This method can be used to relatively calibrate any number of microphones in an array to one common reference.

Figure 5 shows visually how the desirable frequency response function $H_{cal,12}$ is obtained by means of ratios of cross spectra, $G$, or microphone output, $\hat{e}$.

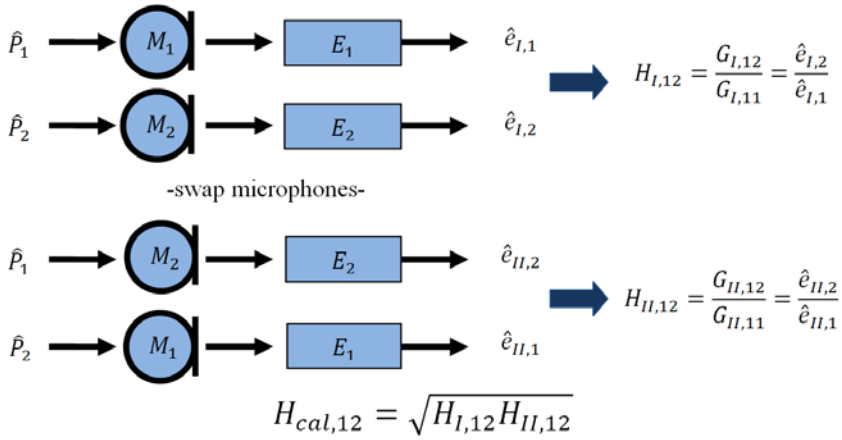


Figure 5. The process of finding a relative calibration between two microphones $M_1$ and $M_2$ with electronic responses $E_1$ and $E_2$ from pressure stimuli of $\hat{P}_1$ and $\hat{P}_2$.

Two laboratory G.R.A.S type 40BE free-field microphones with 26CB type preamplifiers were calibrated multiple times using the method depicted in Figure 5 to determine the transfer function calibration. A G.R.A.S. 42 AE type low-frequency calibrator was used as an acoustic source because of the ease by which the exact switch of sensor locations is performed. Figure 6 shows five overlaid plots of the relative phase and relative magnitude of the calibration. It is

interesting to notice that relative phase difference between the two microphones at 100 Hz is > 3°. However, the variation in phase is very small between trials, < 0.02°. We can then say that, with the calibration, these microphones are phase matched to < 0.02° for 10 Hz to 100 Hz for this exact setup. It is the similarities between trials that determine how effective the calibration is. Similar results are seen for magnitude calibration which results in calibration variations of <0.06 dB for 10 Hz to 100 Hz.

It should be noted that slight variations in environment will affect the calibration in this frequency range and in general, calibrations are only valid for the exact conditions in which they were obtained. When attempting to calibrate for a measurement, the calibration should occur in conditions closely approximating that of the measurement. Individual microphones and microphone pairs will vary.

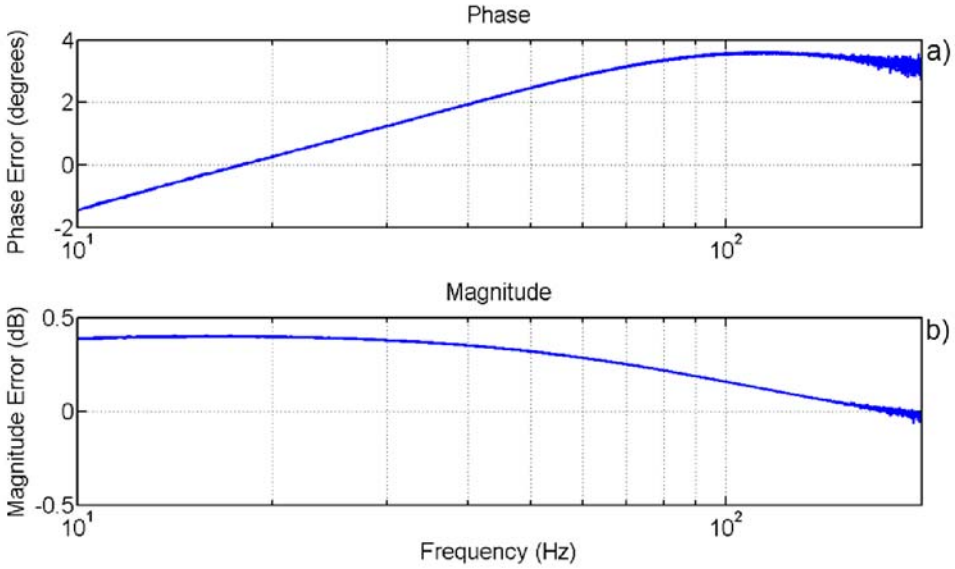


Figure 6. Five overlaid phase (a) and magnitude (b) calibrations relating two microphones.

As a point of interest, the relative phase and magnitudes between each of the sensors used in the experiment are given in Figure 7.

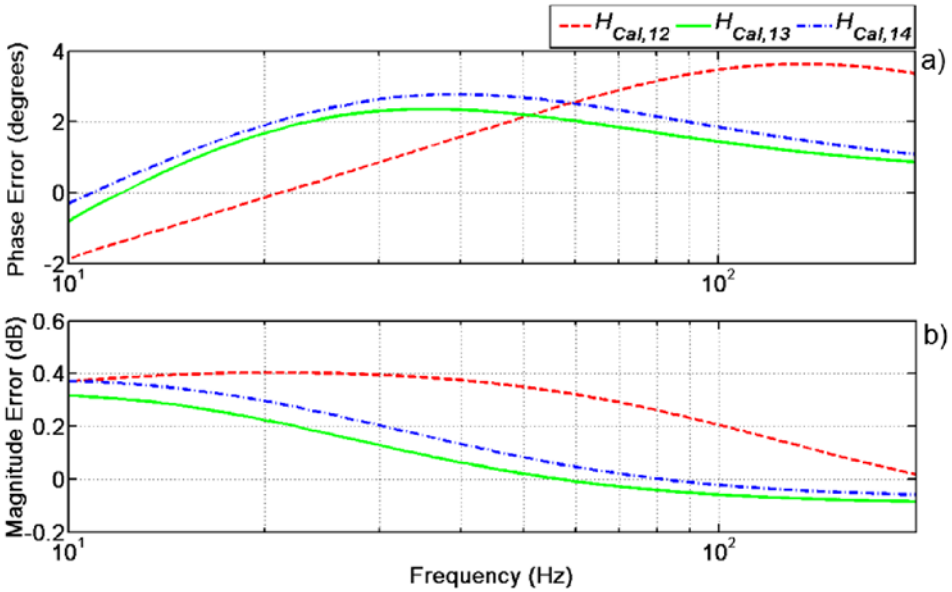


Figure 7. Phase (a) and magnitude (b) transfer functions for the microphones used in the experimental array.

The transfer function $H_{cal,12}$ of Figure 7 is for the same microphone pair, calibrated a separate day, that was shown in Figure 6. These two calibrations are overlaid in Figure 8 to more explicitly show the difference between them. The effective response of the microphone has changed slightly between calibrations and it is not simply a DC shift in magnitude; there has been a shift of the break-point, or roll off, between these calibrations. A challenge of this type of calibration is the tendency for it to drift with slight variations through the duration of the test due to atmospheric field effects. This variation over time/conditions may be equally, if not more, important than our ability to calibrate with great repeatability. In other words, the fact that we can calibrate our microphones to nearly an order of magnitude tighter than reported by the manufacturer may be useless if the test conditions vary from the calibration conditions.

In fairness to G.R.A.S., who have been very helpful in this process, it should be noted, that this particular microphone pair in Figure 8 shows more overall error (Δ5°, Δ0.5 dB) than is typical for these types of sensors. These sensors have been used in multiple experimental setups and it may be that frequent use and 'gentle' abuse may account for the dramatic swings in phase and magnitude response of this pair. Generally these microphones have a "flat" response down at 100 Hz.

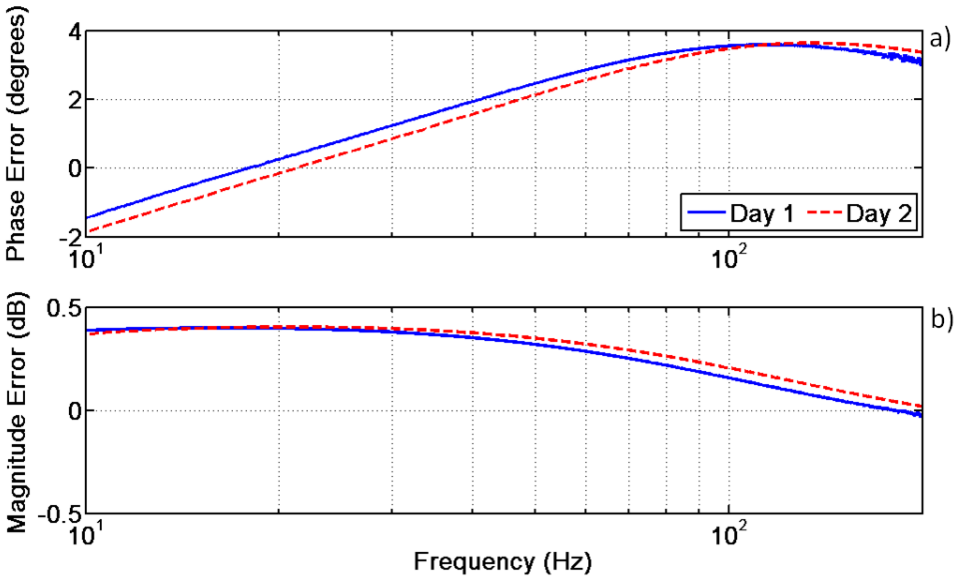


Figure 8. Phase (a) and magnitude (b) transfer functions for the same microphone pair on two separate days. There were approximately 2 weeks between the calibration times.

## EXPERIMENT

An ideal test of the effectiveness of the calibration in improving angle and magnitude errors in measuring acoustic intensity would be to rotate an array of sensors in a plane-wave field and compare the measured intensity with the known intensity of the plane-wave field.

To approximate a plane-wave field, a loudspeaker was set far enough from the array that the diverging waves appear nearly planar over the size of our measurement area. Our frequency range of interest is on the order of tens of Hz and requires either an anechoic chamber with sufficiently deep wedges, or an outdoor measurement to eliminate a standing wave field. The experimental setup is shown in Figure 9. Notice that between the loudspeaker source and microphone array is a concrete sidewalk. A JBL EON 500 series subwoofer was set about 10 m from an intensity probe mounted atop an Outline ST2 turntable. White noise was generated and output by the speaker and recorded at the probe microphones via a custom LabVIEW program. After each 15-second measurement, the turntable was rotated approximately 5° and the measurement was repeated. This process was repeated until 120° of rotation was obtained (120° matches with lines of symmetry of the intensity probe array).

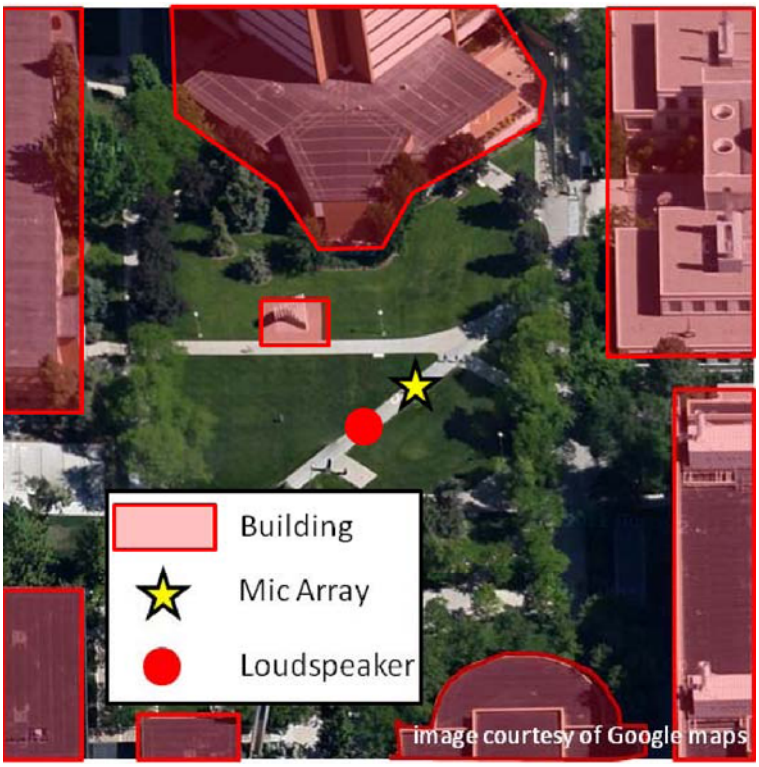


Figure 9. Top-down view of experimental setup.

There are known errors inherent in this experimental design. Although an outdoor location was chosen to reduce the presence of standing waves, due to the large wavelengths involved it was possible some standing waves developed between buildings. The presence of noise from building ventilation systems and passersby was occasionally present. Also, because the environment was not anechoic, there are ground/building reflections that cause interference nulls at the probe. To eliminate interference nulls in the vertical direction within the band of interest, the speaker and probe were placed low to the ground (approx. 0.5 m high). Apart from moving the ground interference null beyond the frequencies of interest, placing the subwoofer near the ground gave approximate doubling of acoustic pressure and improved the signal-to-noise ratio. Figure 10 shows the average sound pressure level, SPL, for each microphone over all angles of rotation. It appears that around 30 Hz, the signal flattens out to what is presumed to be “noise”, both electronic and environmental.

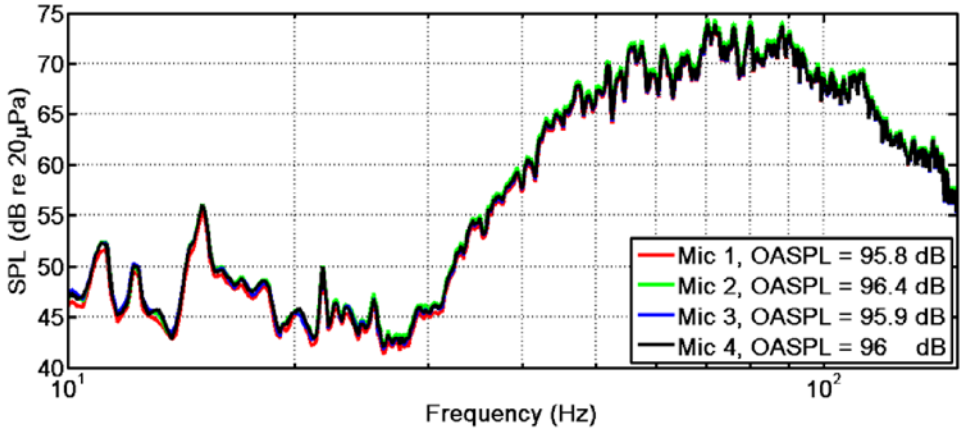


Figure 10. Average SPL for each of the four microphones used during the test

The intensity probe used in this experiment consisted of four 6.35 mm microphones in a tetrahedral configuration with all four of the preamps parallel to each other and the microphone diaphragms faced upwards. Figure 11 depicts an aluminum microphone mount which was manufactured to hold the microphones rigidly throughout the experiment such that a 2.54 cm diameter sphere would circumscribe the centers of the diaphragms.

Figure 11. Four 6.35 mm microphones mounted in a regular tetrahedral arrangement.

## RESULTS

The data have been analyzed both with and without the switching technique calibration applied to the results. The plots in Figure 12 show the directional error for un-calibrated (red) and calibrated (blue) microphones for various angles of rotation. The polar plot angles show the angle of rotation of the multidimensional probe and the rings of constant radius are the angle error. This analysis has multiple references to various angles. To be clear, phase error is a part of the calibration but is not otherwise reported in the results, rotational angle of the array is the angle of the polar plot, and the reported directional error (degree error of locating the source) is indicated by the concentric circles of the polar plot. For example, in Figure 12 for $f$=100 Hz at a probe rotation of 120°, there was 50° of error in locating the source. The calibration improves this result by nearly 45°. It is interesting to notice that the error at 0° and 120° rotation angle are not equal. This is because calibrations differ between the four microphones under test and the importance of each microphone in the calculation of the intensity varies with the rotation.

It is easier to consider the overall effect of the calibration by looking at Figure 13 which depicts the average error from all measurements as a function of frequency. In this experiment the source and receiver were spaced by approximately 10 m. At this distance, 5°, 10° and 20° error correspond to 0.87, 1.7, and 3.4 m error in estimating the location of the source. An area of future research may be to investigate the relatively smooth decrease in angle accuracy below 45 Hz for the calibrated curve. Some of the error may rise from the poor signal-to-noise ratio at these frequencies (see Figure 2.11). However, slight errors in calibration cannot yet be discounted.

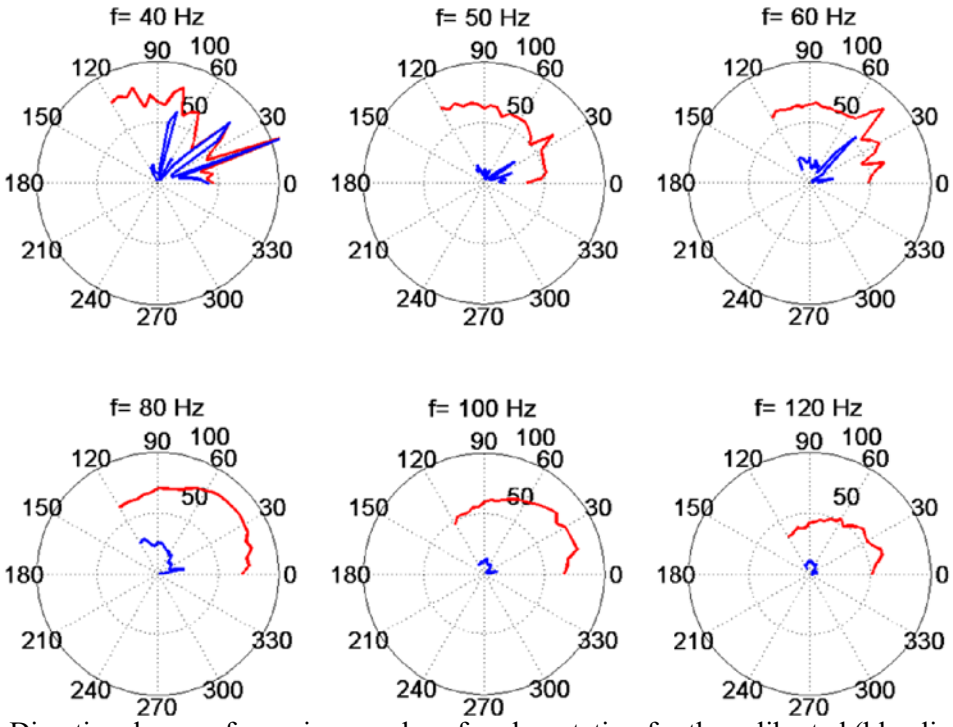


Figure 12. Directional errors for various angles of probe rotation for the calibrated (blue line) and un-calibrated microphones (red line).

Figure 13(a) shows the average angle error as a function of frequency for each of the measurements performed. As the frequency drops to about 30 Hz, the error between the calibrated and non-calibrated calculations is negligible and is centered around 90°. Below 30 Hz may be in the noise floor of the measurement as seen in Figure 12. As the maximum error one can achieve is 180° (pointing directly away from the source) and the minimum error is 0° (pointing directly towards the source), it stands to reason that the average error of this “noisy” data is in the middle at 90° (pointing neither towards or away from the source).

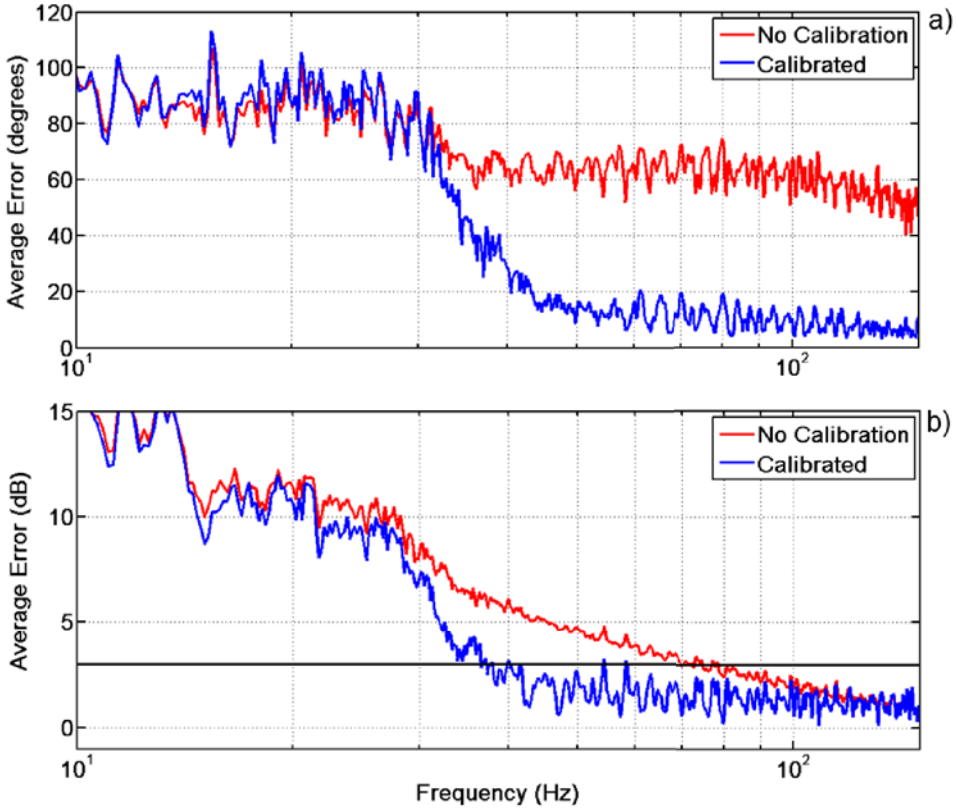


Figure 13. Average angle error (a) of the polar plots in Figure 12 and average intensity magnitude error (b) of the polar plots in Figure 15.

Non-dimensionalized scaling of Figure 13 is given in Figure 14 which relates the angle and magnitude error to *kd*, wavenumber by microphone separation distance.

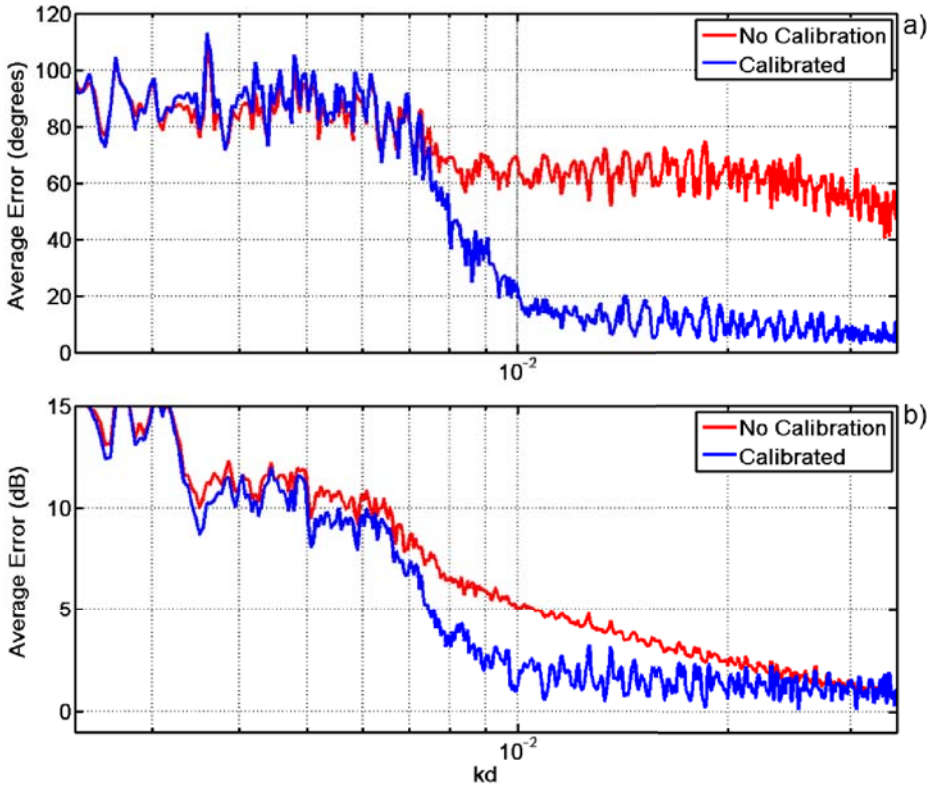


Figure 14. A kd scaled plot of Figure 13

Also a matter of interest is the accuracy of these sensors in measuring the magnitude of the acoustic intensity. Figure 13(b) shows average intensity error in decibels for the angles in the experiment and suggests that above 40 Hz we can expect less than 3 dB error for our calibrated transducer setup. If we consider 3 dB to be the cut-off value, we have extended the range of the probe from 80 Hz to 40 Hz. This factor of 2 increase in bandwidth on a *kd* scale can applied to future probe designs.

Although there appears to be a bias error for the calibrated intensity error, upon closer inspection we see that it is a gently sloping curve that continues to approach zero as frequency increases. It is likely that slight variations in calibrations are to blame, and seems plausible from the data of Figure 4. However, it is likely not possible to prove this concretely with the present results. The reference source for this error analysis is the time averaged intensity of an acoustic plane wave: $< I_{plane} >= \frac{p_{rms}^2}{\rho_0 c}$ using the mean-square pressure of the four microphones. It is interesting to notice that as frequency increases, the impact of the calibration decreases. This is because increasing frequency means more acoustic phase separation between microphones and therefore the microphone phase error becomes less significant relative to the acoustic phase.

The magnitude error for measuring acoustic intensity is found in Figure 15. As was seen with the directional errors, there is a general improvement to the calculation by application of the calibration. At 120 Hz however, we see approximately equal error for the calibrated and un-calibrated cases but the angle of incidence is important when deciding if the calibrated or un-calibrated signal is better. This is likely due to one or more microphones having faulty phase

calibrations at this frequency. Just as the calibration drifted slightly in Figure 8, there may be drift between laboratory calibration and outdoor experiments.

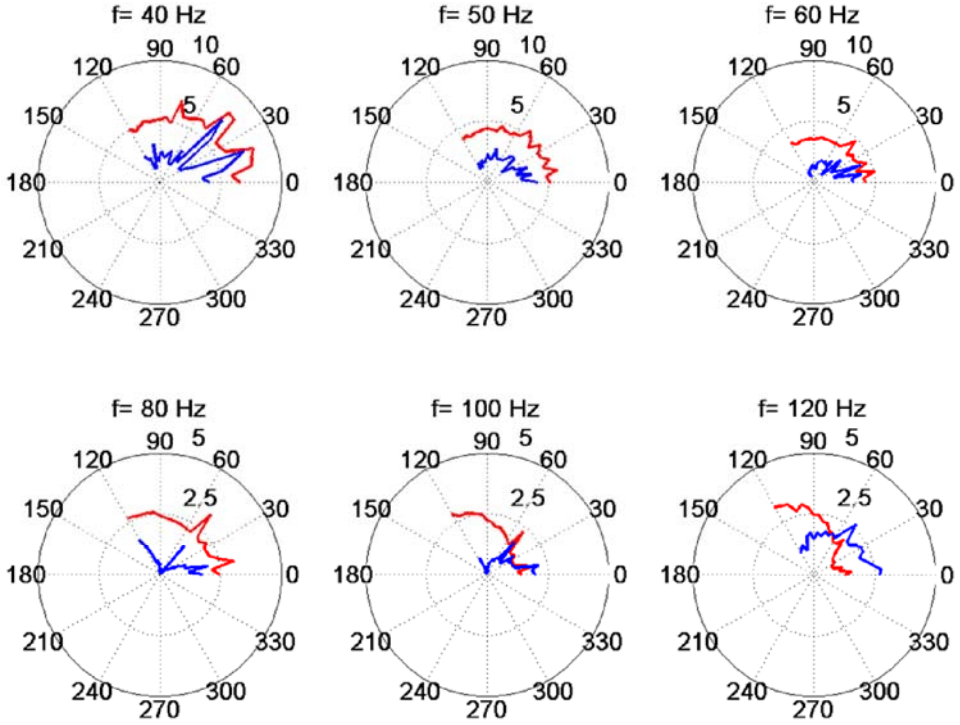


Figure 15. Magnitude error for measuring acoustic intensity for the calibrated result (blue line) and the un-calibrated result (red line).

## SUMMARY

Transfer function calibrations have been obtained for a microphone set and improve the low-frequency response of an intensity probe. The calibrated microphones can achieve variations in phase and magnitude matching of <0.02° and <0.06 dB on a given day. However the stability of these calibrations is questionable and therefore these tight tolerances are not recommended to use as guidelines when deciding microphone spacing to measure a specific frequency range until day to day variation of a sensor set is known and accounted for.

For an outdoor measurement, and at various angles of incidence, the acoustic intensity was measured resulting in error plots showing the ability of the probe to determine the location and intensity of the source. The application of the transfer function calibration improved both direction and magnitude measurements over the frequency range of 30 Hz to 100 Hz. Directional error of the intensity array was improved by ~40 degrees for 40 Hz to 100 Hz and intensity magnitude error also improved to be ~<3 dB for the same bandwidth. On a *kd* scale, this allows the usable range of the probe to be lowered to *kd*=8E-3 from 2E-2.

## SUGGESTIONS FOR FUTURE WORK

Further experiments to confirm the usefulness of these calibrations may be more successfully achieved in a low-noise, half-space environment, such as a very large parking lot or a location such as the Bonneville Salt Flats of Utah. These locations will minimize error sources and give more insight into the next steps in developing these probes. For continued research it may be equally effective, yet simpler, to consider a two-microphone intensity probe at a single angle of

incidence. Also, purchase or development of a low-frequency driver[14] capable of large amplitudes at infrasonic frequencies would be of interest for future work.

Further investigation into the stability of the relative calibration for a microphone set as affected by variations in temperature, pressure, time, rocket environment, etc. may enable one to account for it in the calibration process. For example, it has been seen in laboratory measurements (not reported here) that when a calibration is performed, there is a "warm-up" time for the sensor to achieve a steady state response. Research by another student of Brigham Young University, Ken Bostwick, has found that for any given day, there may be a 0.5° shift at a discrete frequency, say 100 Hz, in the calibration before a "steady state" response is achieved. This understanding applied in the lab calibration and the field measurement increases the effectiveness of the calibration.

Finally, it is presumed that if the same sensors as used to produce Figure 14 were used in another test with a separation distance twice as large, the *kd* plot would look the same, but the frequency plot (as in Figure 13) would show a low-frequency bandwidth cutoff at half of that found previously. The accuracy/linearity of this *kd*-scaling should be checked and may uncover other factors that influence the calibrated intensity measurement at low frequencies.

## ACKNOWLEDGMENTS

This work has been supported by NASA as part of a phase II SBIR awarded to Blue Ridge Research and Consulting for development of an energy-based acoustic measurement system for rocket noise. (Proposal No. 09-2 O2.02 – 8697)

## REFERENCES

[1] K. Eldred, in *Acoustic Loads Generated by the Propulsion System, NASA SP-8072* (1971).
[2] G. Pavic, "Measurement of sound intensity," J. Sound Vib. **51**, 533-545 (1977).
[3] F. Fahy, "Measurmet of acoustic intensity using the cross-spectral density of two microphone signals," J. Acoust. Soc. Am **62**, (1977).
[4] ANSI, "Instruments for the measurement of sound intensity, s1.9-1996," (1996).
[5] *Sound intensity* (Brüel and Kjær, Denmark, 1993).
[6] *Microphone handbook* (Brüel & Kjær, 1996).
[7] (G.R.A.S., http://www.grasinfo.dk/documents/pd_40BI_ver_07_09_05.PDF), Vol. 2012.
[8] S. Gade, *Sound intensity (theory)* (Brüel & Kjaer, 1982).
[9] J. Y. Chung and D. A. Blaser, "Transfer function method of measuring acoustic intensity in a duct system with flow," J. Acoust. Soc. Am **68**, 1570-1577 (1980).
[10] K. H. Miah and E. L. Hixon, "Design and performance evaluation of a broadband three dimensional acoustic intensity measuring system," J. Acoust. Soc. Am **127**, 2338-2346 (2010`).
[11] J. Y. Chung, "Cross-spectral method of measuring acoustic intensity without error caused by instrument phase mismatch," J. Acoust. Soc. Am **64**, 1613-1616 (1978).
[12] G. Krishnappa, "Cross-spectral method of measuring acoustic intensity by correcting phase and gain mismatch errors by microphone calibration," J. Acoust. Soc. Am **69**, 307-310 (1981).
[13] P. Kitech and J. Tichy, "Intensity probe obstacle effects and error of the transfer function technique to calibrate acoustic intensity measurements," Proceedings of Inter-noise 82, 1982, pp. 695-698.
[14] J. Park, M. Garces and B. Thigpen, "The rotary subwoofer: A controllable infrasound source," J. Acoust. Soc. Am **125**, 2006-2012 (2009).